Hindawi
International Journal of Photoenergy
Volume 2023, Article ID 8891052, 8 pages
https://doi.org/10.1155/2023/8891052

*Research Article*

# Scaled Conjugate Gradient Artificial Neural Network-Based Ripple Current Correlation MPPT Algorithms for PV System

**Abdullah M. Noman**,[1] **Hamed Khan**,[2] **Hadeed Ahmed Sher**,[2] **Sulaiman Z. Almutairi**,[1] **Mohammed H. Alqahtani**,[1] **and Ali S. Aljumah**[1]

[1]*Electrical Engineering Department, College of Engineering, Prince Sattam Bin Abdulaziz University, Al-Kharj, Saudi Arabia*
[2]*Faculty of Electrical Engineering, GIK Institute of Engineering Sciences and Technology, Topi 23460, Pakistan*

Correspondence should be addressed to Abdullah M. Noman; a.noman@psau.edu.sa

Received 20 March 2023; Revised 7 May 2023; Accepted 3 June 2023; Published 21 June 2023

Academic Editor: Francesco Riganti-Fulginei



This article proposes a hybrid scheme of maximum power point tracking (MPPT) based on artificial neural network (ANN) and ripple current correlation (RCC). ANN model is established using the data generated through RCC MPPT. Scaled conjugate gradient ANN is applied to gauge the performance improvement. The proposed scheme is validated through simulations. For this, the proposed system is applied to three different environmental scenarios which are standard testing condition of a PV module, under variable irradiance condition, and variable temperature condition. It is established that the proposed system is well capable of tracking the maximum power point under various test conditions.

## 1. Introduction

Solar photovoltaic (PV) energy is an important area of interest among the energy producers. With rapid technological progress, the prices of PV modules have declined substantially, and hence, the power generation through PV is witnessing exponential growth [1]. The emergence of large-scale grid-connected solar PV systems has posed substantial challenges to power networks in terms of flexibility, efficiency, and energy balance [2, 3]. The output characteristics of PV modules are functions of irradiance and temperature and vary nonlinearly over the range of operating voltage. This requires algorithmic calculations to operate the PV module at the maximum power it can generate under any given environmental condition [4, 5]. These algorithms are termed as maximum power point tracking (MPPT) algorithms. A categorization and thorough list of numerous MPPT algorithms are presented in [6, 7]. In addition, the performance assessment of commercially used MPPT techniques such as hill climbing (HC), perturb and observe (P&O), and incremental conductance (InC) is done in [8]. Even though these approaches are widely used and can track maximum power point (MPP) under steady weather conditions, each of them has its own set of drawbacks as listed in [9–12].

Artificial intelligence control has been used in a wide range in many fields such as machine drive control and power electronics control. The use of fuzzy logic controllers has been increased over the last decade because of its simplicity, ability to deal with imprecise inputs, lack of need for an accurate mathematical model, and ability to handle nonlinearity. Due to their robustness, simple design, and capability of dealing with uncertain weather design, artificial intelligence-based techniques such as the fuzzy logic controller (FLC), artificial neural networks (ANNs), and adaptive neurofuzzy inference systems (ANFIS) are adopted as a controller to extract the maximum power that the PV modules produce [13–15]. Moreover, these algorithms do not require prior knowledge of the exact model of the system [16–18]. FLC-based MPPT techniques can be evaluated by trial and

error process. The design of FLC MPPT techniques is limited due to the long time consumed to generate the suitable membership functions [19, 20].

Artificial neural network (ANN) is among the modern methods to effectively track the maximum power point [21]. Like other MPPT methods, the performance of ANN-based MPPT system is categorized in terms of accuracy, convergence speed, implementation difficulty, stability, cost, and electronics equipment requirement [22]. The ANN system is based on a biological network of the human brain. It is trained and evaluated using the nonlinear characteristics of the PV system. Thus, it learns to alter the behavior of the solar power system based on the inputs such as current, voltage, and irradiance [23]. ANN has a number of advantages, including outstanding accuracy in modeling and solving nonlinear processes [24]. An artificial neural network (ANN) can be employed to improve the speed and accuracy of solar power system modeling and forecasting [25]. It has been demonstrated to have a quicker response time and less oscillation in the vicinity of MPP [26].

A survey of the literature reveals that little work has been done with the Levenberg-Marquardt (LM), Bayesian regularization (BR), and scaled conjugate gradient (SCG) variants of ANN algorithms [27]. In the literature and published publications, there are some studies based on comparative examinations of different MPPT variants for solar PV systems, and there still exists a substantial research gap. To bridge this research gap, ANN-based algorithms with the RCC method for MPPT solar energy harvesting are proposed in this article. A comprehensive strategy is used to analyze the performance characteristics of the SCG-ANN algorithms using training, validation, and analysis of real data sets of solar irradiance, temperature, and generated voltage. A simulated model is created using MATLAB/Simulink, which provides a clear scenario for the deployment of ANN MPPT algorithms in solar PV systems.

## 2. State of the Art of ANN and MPPT

A neural network is an information processing system [28]. Imported data is used to train ANN, which is known as supervised learning or training. ANN, like the human brain, is made up of a vast number of neurons [29]. During the training phase, the consequences will be adjusted in order to make precise predictions, and the weight quantities will remain constant until the error surpasses the allowable value [30]. The two-layer ANN model is demonstrated in its most basic form as depicted in Figure 1. Corresponding to that of the neural network on the right side, the inputs might be merged into the network at different moments. Complete input-output parameter data sets are separated into two groups, one with a greater proportion of data points called the training data set, and the other with a lower percentage of data points called the test data set, which is used to train a neural network. In the second group, the remaining data points are utilised to check what the neural network has learned, referred to as the validation data set [31]. The neural network's input-output parameters and their training data points are imported. This network will be conditioned

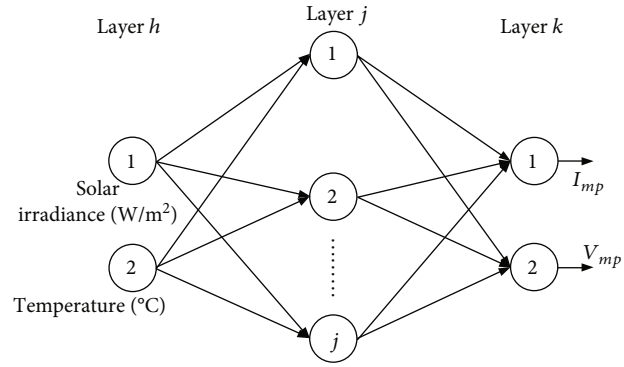


Figure 1: Structure of a two-layer ANN.

until an allowed error occurs. After receiving an actual error, by importing the input parameters from the validation data set and predicting the corresponding output parameter values, the qualified network is validated.

These extended validation dataset output parameter values are linked to the genuine validation data set output parameter values. If the difference between the real and projected outcomes is smaller than the maximum allowed, the qualifying neural network can be proposed as the best prediction neural network.

## 3. Modeling of Photovoltaic System

A PV module is made up of PV cells that are coupled in series and parallel. The series and parallel combination would enhance the voltage and current of the array. A similar electrical circuit of a solar cell comprised of a current source, diode, and series and parallel resistances to best replicate the actual characteristics of the solar cell. The series and parallel resistances represent the leakage current losses and contact resistance losses in a solar cell, respectively. Figure 2 shows the single-diode model of the single solar cell.

The equation describing the relationship of the solar irradiation with generated current is as follows:

$$I = I_{\text{ph}} - I_o \exp\left(q\left(V_{\text{pv}} + I_{\text{pv}}R_s\right)/\alpha K_b T N_s\right) - 1, \quad (1)$$

where $I_o$ is the diode saturation current and $V_t$ is the thermal voltage whose value is $\alpha \text{K}_b T/q$, where $T$ is the temperature in kelvin, $\text{K}_b$ is the Boltzmann constant, $q$ is the charge on the electron and $\alpha$ is ideality factor.

The P-V and I-V curves for the PV system with uniform irradiation are shown in Figure 3.

## 4. Ripple Correlation Control

Ripple correlation current maximum power point tracking (RC-MPPT) is a technique used in photovoltaic (PV) systems to optimize the amount of power that can be harvested from solar panels. In RCC, a small amplitude ripple current is superimposed on the DC current flowing through the PV module. The voltage response of the module to this ripple current is then monitored and analyzed to determine the maximum power point (MPP) of the module. The MPP is

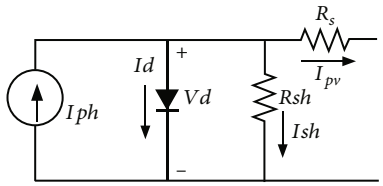


Figure 2: Single-diode model of the single solar cell.

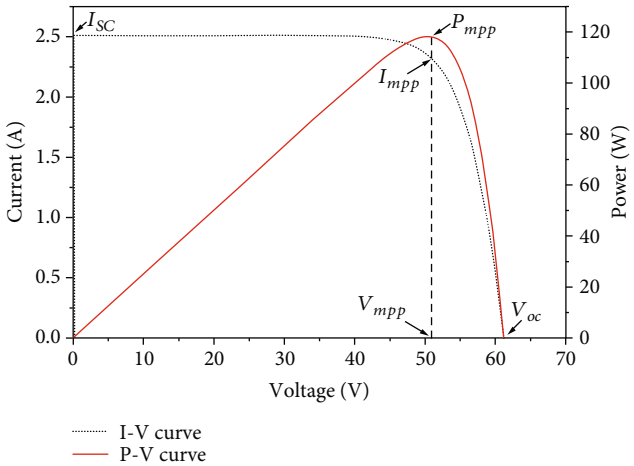


Figure 3: P-V and I-V curves under uniform irradiation.

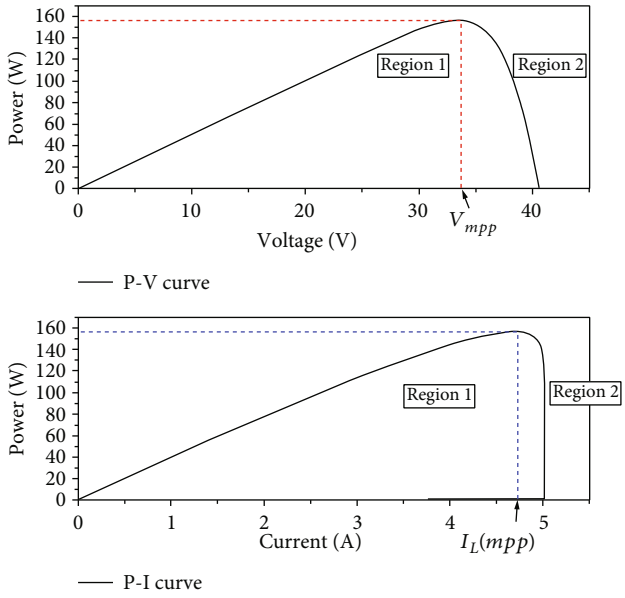


Figure 4: P-V and P-I curves of the module.

the operating point at which the module can deliver maximum power to the load. Once the MPP is determined, the system adjusts the operating point of the PV module to ensure that it operates at the MPP. This is done by varying the load or adjusting the operating voltage of the module. The advantage of RC-MPPT over other MPPT techniques is that it can track the MPP under rapidly changing environmental conditions, such as rapidly changing solar irradiance or shading. It is also more efficient than other techniques as it requires a small amplitude ripple current which can be easily generated and does not consume much power [32, 33].

A great strength of RCC is that it takes the help of inherent ripples of the DC-DC converters that are present due to the switching. To correlate the PV power with the ripple of the inductor current, the RCC technique drives to its MPP without external perturbation [32, 33].

Figure 4 shows the PV array power and inductor average current curve of a boost converter. In this graph, the maximum power corresponds to $P_{\text{mpp}}$ and $I_{L\text{mpp}}$ is the inductor current on which the maximum power is achieved. With the help of the RCC method, the ripple components of the $I_L$ and those of PV power can be correlated. The same can be achieved using the correlation of ripple in the PV voltage and the PV power to decide about the point of operation of the MPP.

Since there is one peak in the P-I and P-V curves during uniform irradiance, hence, the P-V curve will be divided into two regions around the MPP point. The region which is at the left of the MPP contains the point where the ripple of both parameters is in phase, whereas the right region of the MPP is the region where both the parameters are out of phase. The functionality of RCC is based on this principle.

This implies that the product of the time derivative of $I_L$ and the time derivative of power ($P$) is positive in region 1 and negative in region 2. This is shown in Equations (2) and (3) which leads to the primary form of the RCC control law.

$$\frac{dI_L}{\text{dt}}\frac{dP}{\text{dt}} > 0, \tag{2}$$

$$\frac{dI_L}{\text{dt}}\frac{dP}{\text{dt}} < 0. \tag{3}$$

The value of $I_L$ can be adjusted by changing the duty cycle "$d$" of the switch in DC-DC converter. The inductor current increases and decreases with the duty cycle. The duty cycle can be expressed as shown in Equation (4), where $k$ is a positive constant gain.

$$d = k\int_{\cdot}\left(\frac{dP}{\text{dt}}\right)\left(\frac{dV}{\text{dt}}\right)\text{dt}. \tag{4}$$

Equations (2) and (3) can vary widely due to the variation in the ripple of $I_L$. The other limitation associated with correlating the PV power ripple with the inductor current ripple is that it can work under low frequency. To avoid such variation and to ensure work under a high-frequency range, one can use the voltage variation in the PV panel to correlate with PV power instead of inductor current ripple. Another variant is the signum function of the time derivative. Taking the time derivative as input to the signum function means that the sign information of the derivative can be used. This will be a lot easier to implement since the sign function can eliminate the noise caused by the differentiation. The

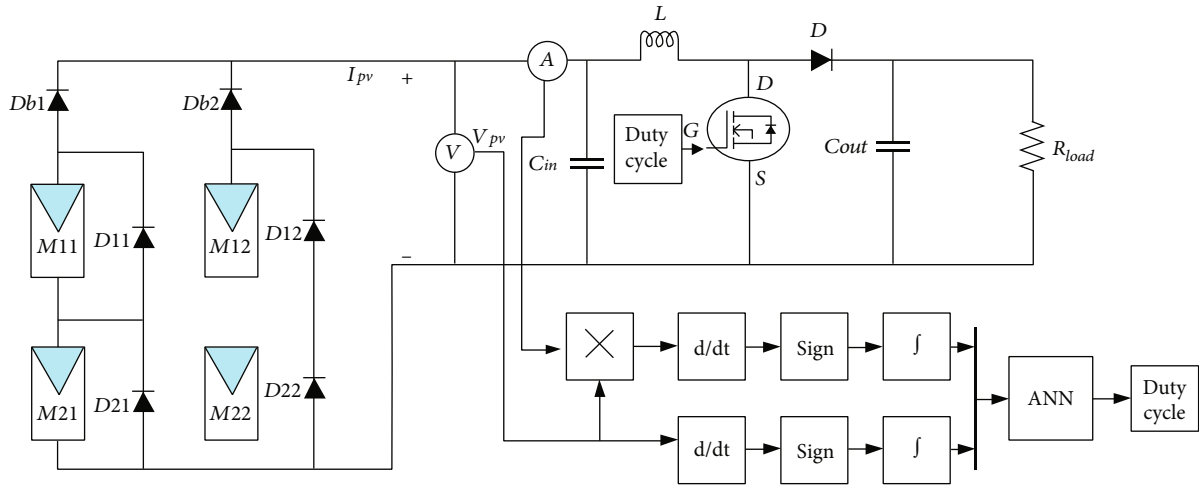


Figure 5: The block diagram of the overall system.

signum function is shown in Equation (5), and the modified control RCC law is shown in Equation (6).

$$\text{sign}(x) = \begin{cases} -1 & \text{When x} < 0, \\ 0 & \text{When x} = 0, \\ 1 & \text{When x} > 0, \end{cases} \tag{5}$$

$$d = k\int_{\cdot} \text{sign}\left(\frac{dP}{\text{dt}}\right) \text{sign}\left(\frac{dV}{\text{dt}}\right)\text{dt}. \tag{6}$$

## 5. Proposed MPPT Algorithm

The suggested artificial neural network is built on the RCC principle, where the duty cycle depends on the control law given in the following:

$$d = m\int_{\cdot} \left(\frac{dP}{\text{dt}}\right)\left(\frac{dV}{\text{dt}}\right)\text{dt}. \tag{7}$$

Inputs to the ANN system are the correlation of the time derivative of the voltage ripple across the inductor and the power of the PV system. Data is collected as the environmental condition changes. A comparator in the ANN MPPT subsystem compares the ANN's output voltage $V_{\text{ANN}}$ with the inductor voltage $V_L$. The inductor voltage $V_L$, acts as a reference voltage to the comparator. The duty cycle is generated via a proportional-integral-derivative (PID) controller based on the voltage difference between $V_{\text{ANN}}$ and $V_L$. The gate signal is applied to the pulse width modulated (PWM) generator which drives the dc-dc boost converter.

The ANN algorithm's optimum correlation between the goal and training value guarantees a consistent duty cycle value, thus smoothing the switching of the dc-dc converter. For multidimensional problems, a multilayer feed-forward network is required; therefore, a feed-forward back propagation ANN with three hidden layers with logsig, purelin, and purelin activation functions is employed in this study. There are four neurons in the first, ten in the second, and four in the third. An output neuron with a poslin activation function makes up the output layer as shown in Figure 1. On a heuristic basis, the ideal number of neurons in the hidden layers is found such that the prediction accuracy is acceptable.

Table 1: Specification of PV module at STC 1000 $W/m^2$, air mass (AM) 1.5, 25°C.

| Symbols | Variables | Values |
|---|---|---|
| | PV module | |
| $P_{Mp}$ | Maximum power point | 40 W |
| $V_{\text{OC}}$ | Open circuit voltage | 21 V |
| $I_{\text{SC}}$ | Short circuit current | 2.57 A |
| $V_{\text{MP}}$ | Voltage at MPP | 17 V |
| $I_{\text{MP}}$ | Current at MPP | 2.35 A |
| $N_S$ | No. of series connected cells | 60 |

## 6. Simulation

The proposed ANN-based RCC method is validated in Matlab/Simulink using an array of Soltech ISTH-215-P solar panel as shown in Figure 5. The proposed method can be implemented on various kinds of dc-dc converters like the one reported in [34–36], but for this work, a dc-dc boost converter is adopted as shown in the block diagram. The dc-dc boost converter interfaces a $2 \times 2$ PV array with a resistive load. The converter has an input capacitor $C_{\text{in}} = 1000\,\mu$F, inductor = 50 $\mu$H, and output capacitor $C_{\text{out}} = 47\,\mu$F; load resistance is 140 $\Omega$, while the switching frequency is kept at 20 kHz. The array is equipped with blocking diodes which block any localized current circulation due to string mismatch. The specification of this PV module is given in Table 1. The proposed hybrid MPPT system is trained by varying the temperature and irradiance. To validate the proposed hybrid MPPT scheme, the PV array is subject to standard testing condition (1000 $W/m^2$ at 25°C cell temperature)

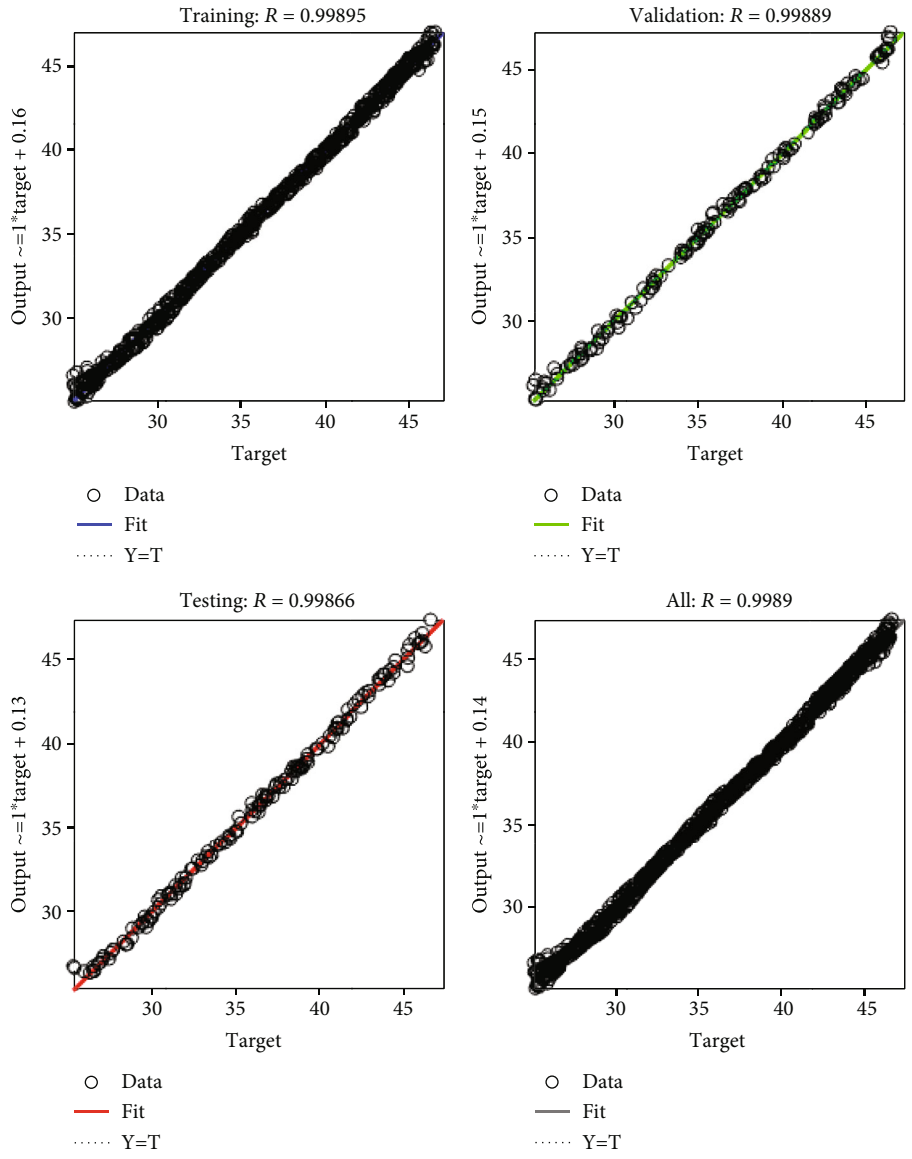


Figure 6: Regression plot for SCG algorithm.

and two variable environmental conditions with irradiance and temperature variation (as shown in the corresponding figures). The effectiveness of each hybrid MPPT algorithm is verified using one among the power, voltage, current, and duty cycle waveforms.

*6.1. Scaled Conjugate Gradient (SCG).* This variant of ANN is based on the conjugate directions, but unlike other conjugate gradient algorithms, it does not perform a line search on each iteration. The regression plot for this algorithm is depicted in Figure 6, which is smaller than LM and BR algorithms.

The error histogram plot for the SCG algorithm is shown in Figure 7. With this approach, the total error range is from -1.548 to 0.7268. At 150 samples, the mean bin has a near-zero error of 0.00856, which is higher than the mean bin of the LM and BR ANN algorithms.

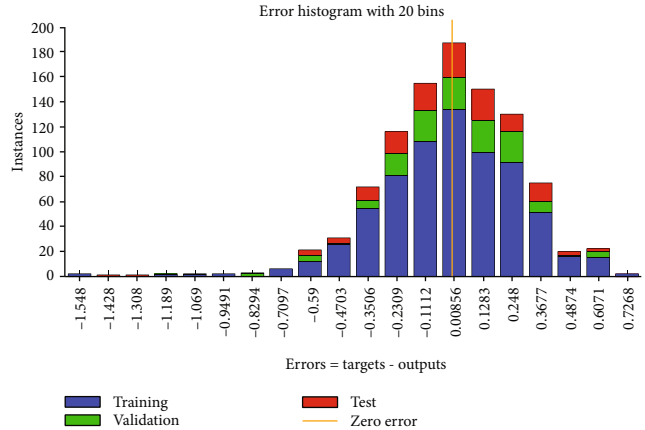


Figure 7: Error histogram plot for SCG algorithm.

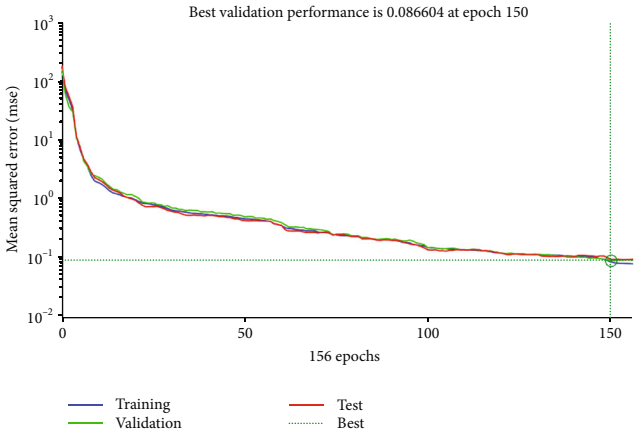


Figure 8: Performance plot for SCG algorithm.

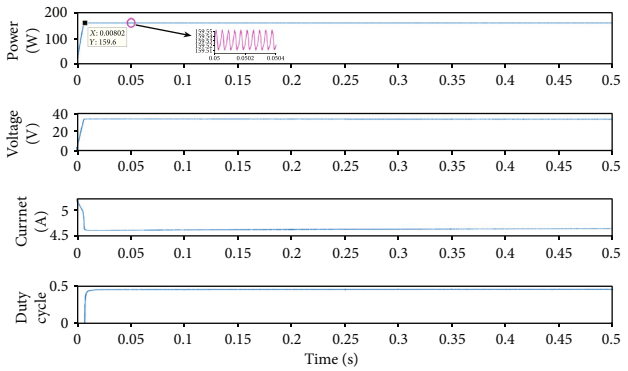


Figure 9: Test 1: performance of proposed SCG-ANN-based RCC algorithm under standard testing conditions (STC).

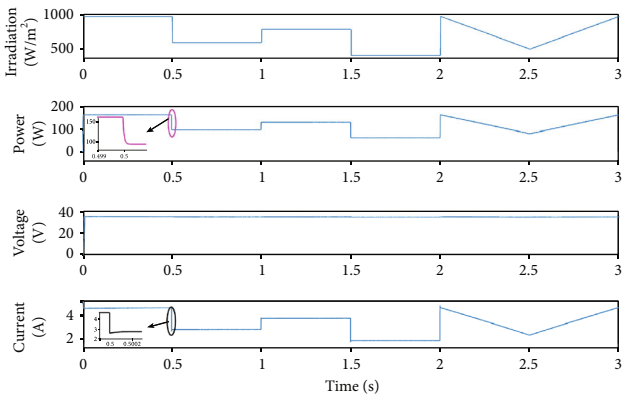


Figure 10: Test 2: performance of proposed SCG-ANN-based RCC algorithm under variable irradiance condition.

The performance plot for the SCG algorithm is shown in Figure 8. According to the simulation result, the best performance of the training data set is with MSE equal to 0.086604 at 1000 epochs.

The SCG-ANN is also trained at STC condition as shown in Figure 9. The algorithm tracking speed is slower than both the LM and BR variants of the ANN RCC algorithm. However, the target is achieved satisfactorily with this ANN variant.

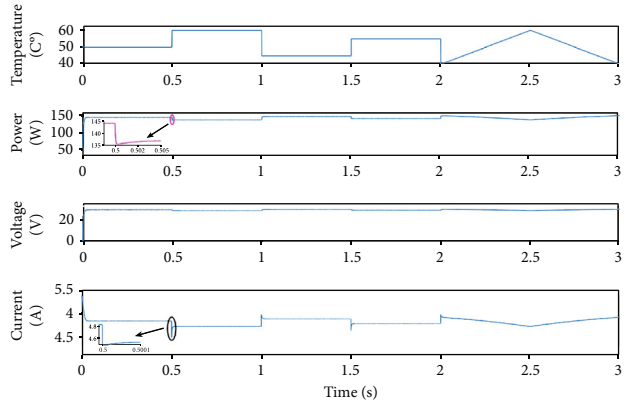


Figure 11: Test 3: performance of proposed SCG-ANN-based RCC algorithm under variable temperature condition.

The RCC based on SCG-ANN MPPT is subjected to a test under variable irradiance condition as shown in Figure 10. Because irradiation changes the MPP, the RCC-based SCG algorithm keeps a close check on the new MPP. It does, however, follow the new MPP more slowly than the BR and LM algorithms.

The system is trained with variable temperature and constant irradiance condition as shown in Figure 11. The corresponding performance showcases the tracking of MPP with negligible undershooting.

## 7. Discussion

The proposed system works best under the small and medium-scale PV systems. The proposed scheme adopts the ANN-based scheme, and therefore, for all large-scale applications, it demands high-speed computing systems which limits its use to only the small- and medium-scale PV plants. It is seen in the simulation that the proposed system treats the PV array as a two-port network and that it is able to track the maximum power out of the available power. This implies that the variations in PV panel characteristics and mismatch have no impact on the performance of the proposed algorithm.

## 8. Conclusion

In this paper, three hybrid RCC MPPT methods are presented using three different variants of ANN. The ANN variants applied on the proposed hybrid scheme are the LM, BR, and SCG. All the methods yielded acceptable results, with the LM method having the best performance, yielding an efficiency of 99.875% and tracking time of just 6.88 ms. The presented methods and their results form the bottom line for the future work on the RCC algorithm.

## Data Availability

Data will be available upon request.

## Conflicts of Interest

The authors declare no conflict of interest.

## Acknowledgments

The authors extend their appreciation to the Deputyship for Research & Innovation, Ministry of Education in Saudi Arabia for funding this research work through the project number (IF2/PSAU/2022/01/23150).

## References

[1] M. Bolinger and G. Bolinger, "Land requirements for utility-scale PV: an empirical update on power and energy density," *IEEE Journal of Photovoltaics*, vol. 12, no. 2, pp. 589–594, 2022.

[2] Z. Dalala, M. Al-Omari, M. Al-Addous, M. Bdour, Y. Al-Khasawneh, and M. Alkasrawi, "Increased renewable energy penetration in national electrical grids constraints and solutions," *Energy*, vol. 246, article 123361, 2022.

[3] D. S. Nair and T. Rajeev, "Impact of reverse power flow due to high solar PV penetration on distribution protection system," in *Sustainable Energy and Technological Advancements*, pp. 1–13, Springer, 2022.

[4] A. Hussain, H. A. Sher, A. F. Murtaza, and K. Al-Haddad, "Revised perturb and observe approach for maximum power point tracking of photovoltaic module using finite control set model predictive control," in *2019 IEEE 28th International Symposium on Industrial Electronics (ISIE)*, pp. 962–967, Vancouver, BC, Canada, 2019.

[5] I. Pervez, I. Shams, S. Mekhilef, A. Sarwar, M. Tariq, and B. Alamri, "Most valuable player algorithm based maximum power point tracking for a partially shaded PV generation system," *IEEE Transactions on Sustainable Energy*, vol. 12, no. 4, pp. 1876–1890, 2021.

[6] N. Karami, N. Moubayed, and R. Outbib, "General review and classification of different mppt techniques," *Renewable and Sustainable Energy Reviews*, vol. 68, pp. 1–18, 2017.

[7] R. Ahmad, A. F. Murtaza, and H. A. Sher, "Power tracking techniques for efficient operation of photovoltaic array in solar applications - a review," *Renewable and Sustainable Energy Reviews*, vol. 101, pp. 82–102, 2019.

[8] A. F. Murtaza, H. A. Sher, M. Chiaberge, D. Boero, M. De Giuseppe, and K. E. Addoweesh, "Comparative analysis of maximum power point tracking techniques for PV applications," in *INMIC*, pp. 83–88, Lahore, Pakistan, 2013.

[9] P. N. Tawiah-Mensah, J. Addison, S. Dei Oppong, and F. B. Effah, "An improved perturb and observe maximum power point tracking algorithm with the capability of drift avoidance in PV systems," in *2022 IEEE PES/IAS PowerAfrica*, pp. 1–5, Kigali, Rwanda, 2022.

[10] M. Hebchi, A. Kouzou, and A. Choucha, "Improved incremental conductance algorithm for mppt in photovoltaic system," in *2021 18th International Multi-Conference on Systems, Signals & Devices (SSD)*, pp. 1271–1278, Monastir, Tunisia, 2021.

[11] I. Pervez, A. Sarwar, A. Pervez, M. Tariq, and M. Zaid, "An improved maximum power point tracking (MPPT) of a partially shaded solar PV system using PSO with constriction factor (PSO-CF)," in *Advances in Electromechanical Technologies. Lecture Notes in Mechanical Engineering*, pp. 499–507, Springer, 2021.

[12] I. Pervez, A. Sarwar, A. Alam, M. Tariq, R. K. Chakrabortty, and M. J. Ryan, "An MPPT method using hybrid radial movement optimization with teaching-learning based optimization under fluctuating atmospheric conditions," *Journal of Intelligent & Fuzzy Systems*, vol. 42, no. 2, pp. 807–816, 2022.

[13] C. G. Villegas-Mier, J. Rodriguez-Resendiz, J. M. Álvarez-Alvarado, H. Rodriguez-Resendiz, A. M. Herrera-Navarro, and O. Rodríguez-Abreo, "Artificial neural networks in mppt algorithms for optimization of photovoltaic power systems: a review," *Micromachines*, vol. 12, no. 10, p. 1260, 2021.

[14] P. Verma, A. Alam, A. Sarwar et al., "Meta-heuristic optimization techniques used for maximum power point tracking in solar PV system," *Electronics*, vol. 10, no. 19, p. 2419, 2021.

[15] I. Pervez, A. Pervez, M. Tariq, A. Sarwar, R. K. Chakrabortty, and M. J. Ryan, "Rapid and robust adaptive jaya (ajaya) based maximum power point tracking of a PV-based generation system," *IEEE Access*, vol. 9, pp. 48679–48703, 2021.

[16] C. Larbes, S. A. Cheikh, T. Obeidi, and A. Zerguerras, "Genetic algorithms optimized fuzzy logic control for the maximum power point tracking in photovoltaic system," *Renewable Energy*, vol. 34, no. 10, pp. 2093–2100, 2009.

[17] C. A. Tavares, K. T. Leite, W. I. Suemitsu, and M. D. Bellar, "Performance evaluation of photovoltaic solar system with different MPPT methods," in *2009 35th Annual Conference of IEEE Industrial Electronics*, pp. 719–724, Porto, Portugal, 2009.

[18] A. G. Al-Gizi, A. Craciunescu, and S. J. Al-Chlaihawi, "The use of ANN to supervise the PV MPPT based on FLC," in *2017 10th International Symposium on Advanced Topics in Electrical Engineering (ATEE)*, pp. 703–708, Bucharest, Romania, 2017.

[19] B. Kavya Santhoshi, K. Mohana Sundaram, S. Padmanaban, J. B. Holm-Nielsen, and K. K. Prabhakaran, "Critical review of PV grid-tied inverters," *Energies*, vol. 12, no. 10, p. 1921, 2019.

[20] S. S. Mohammed, D. Devaraj, and T. I. Ahamed, "GA-optimized fuzzy-based mppt technique for abruptly varying environmental conditions," *Journal of The Institution of Engineers (India): Series B*, vol. 102, no. 3, pp. 497–508, 2021.

[21] H. Bouaouaou, D. Lalili, and N. Boudjerda, "Model predictive control and ANN-based mppt for a multi-level grid-connected photovoltaic inverter," *Electrical Engineering*, vol. 104, no. 3, pp. 1229–1246, 2022.

[22] A. Nadeem, H. A. Sher, A. F. Murtaza, and N. Ahmed, "Online current-sensorless estimator for PV open circuit voltage and short circuit current," *Solar Energy*, vol. 213, pp. 198–210, 2021.

[23] C. Basha and C. Rani, "Different conventional and soft computing MPPT techniques for solar PV systems with high step-up boost converters: a comprehensive analysis," *Energies*, vol. 13, no. 2, p. 371, 2020.

[24] I. Chtouki, P. Wira, and M. Zazi, "Comparison of several neural network perturb and observe mppt methods for photovoltaic applications," in *2018 IEEE International Conference on Industrial Technology (ICIT)*, pp. 909–914, Lyon, France, 2018.

[25] M. S. Bouakkaz, A. Boukadoum, O. Boudebbouz, A. Bouraiou, N. Boutasseta, and I. Attoui, "ANN based mppt algorithm design using real operating climatic condition," in *2020 2nd International Conference on Mathematics and Information Technology (ICMIT)*, pp. 159–163, Adrar, Algeria, 2020.

[26] C. R. Algarín, D. S. Hernández, and D. R. Leal, "A low-cost maximum power point tracking system based on neural

network inverse model controller," *Electronics*, vol. 7, no. 1, p. 4, 2018.

[27] I. Khan, M. A. Z. Raja, M. Shoaib et al., "Design of neural network with Levenberg-Marquardt and Bayesian regularization backpropagation for solving pantograph delay differential equations," *IEEE Access*, vol. 8, article 137918, 2020.

[28] D. V. Siva Krishna Rao K, M. Premalatha, and C. Naveen, "Analysis of different combinations of meteorological parameters in predicting the horizontal global solar radiation with ANN approach: a case study," *Renewable and Sustainable Energy Reviews*, vol. 91, pp. 248–258, 2018.

[29] I. M. El-Amin and A.-A. M. Al-Shams, "Transient stability assessment using artificial neural networks," *Electric Power Systems Research*, vol. 40, no. 1, pp. 7–16, 1997.

[30] N. J. Vickers, "Animal communication: when i'm calling you, will you answer too?," *Current Biology*, vol. 27, no. 14, pp. R713–R715, 2017.

[31] K. Pielichowska, J. Bieda, and P. Szatkowski, "Polyurethane/graphite nano-platelet composites for thermal energy storage," *Renewable Energy*, vol. 91, pp. 456–465, 2016.

[32] T. Esram, J. W. Kimball, P. T. Krein, P. L. Chapman, and P. Midya, "Dynamic maximum power point tracking of photovoltaic arrays using ripple correlation control," *IEEE Transactions on Power Electronics*, vol. 21, no. 5, pp. 1282–1291, 2006.

[33] C. Barth and R. C. Pilawa-Podgurski, "Dithering digital ripple correlation control for photovoltaic maximum power point tracking," *IEEE Transactions on Power Electronics*, vol. 30, no. 8, pp. 4548–4559, 2014.

[34] N. A. Hamood-Ur-Rehman, H. A. Sher, A. Al-Durra, and H. M. Hasanien, "Comprehensive analysis and design of a switched-inductor type low inductance-requirement dc-dc buck-boost converter for low power applications," *IET Power Electronics*, vol. 16, no. 7, pp. 1239–1254, 2023.

[35] U. Rafiq, A. F. Murtaza, H. A. Sher, and D. Gandini, "Design and analysis of a novel high-gain dc-dc boost converter with low component count," *Electronics*, vol. 10, no. 15, p. 1761, 2021.

[36] H. Tarzamni, H. S. Gohari, M. Sabahi, and J. Kyyrä, "Non-isolated high step-up dc-dc converters: comparative review and metrics applicability," *IEEE Transactions on Power Electronics*, pp. 1–41, 2023.